

A SEARCH FOR LOW-LUMINOSITY BL LACERTAE OBJECTS

TRAVIS A. RECTOR^{1,2,3,4} AND JOHN T. STOCKE^{1,2,3}

Center for Astrophysics and Space Astronomy, University of Colorado, Boulder, Colorado 80309-0389

AND

ERIC S. PERLMAN

Space Telescope Science Institute, Baltimore, MD 21218

Draft version January 25, 2018

ABSTRACT

Many properties of BL Lacs have become explicable in terms of the “relativistic beaming” hypothesis whereby BL Lacs are FR-1 radio galaxies viewed nearly along the jet axis. However, a possible problem with this model is that a transition population between beamed BL Lacs and unbeamed FR-1s has not been detected. A transition population of “low-luminosity BL Lacs” was predicted to exist in abundance in X-ray-selected samples such as the *Einstein* Extended Medium Sensitivity Survey (EMSS) by Browne & Marchā. However, these BL Lacs may have been misidentified as clusters of galaxies. We have conducted a search for such objects in the EMSS with the ROSAT HRI; and here we present ROSAT HRI images, optical spectra and VLA radio maps for a small number of BL Lacs which were previously misidentified in the EMSS catalog as clusters of galaxies. While these objects are slightly lower in luminosity than other EMSS BL Lacs, their properties are too similar to the other BL Lacs in the EMSS sample to “bridge the gap” between BL Lacs and FR-1 radio galaxies. Also, the number of new BL Lacs found are too few to alter significantly the X-ray luminosity function or $\langle V/V_{max} \rangle$ value for the X-ray-selected EMSS BL Lac sample. Thus, these observations do not explain fully the $\langle V/V_{max} \rangle$ discrepancy between the X-ray and radio-selected BL Lac samples.

Subject headings: BL Lacertae Objects — AGN — Unification Models

1. INTRODUCTION

BL Lacertae Objects are a very enigmatic type of active galactic nucleus (AGN). They are highly luminous (e.g., $\log L_x = 44\text{--}46$ ergs s^{-1} ; Morris et al. 1991, hereafter M91), dominated by a non-thermal, nearly-featureless continuum (which often makes redshift determinations difficult) and exhibit several characteristics indicative of relativistic outflows nearly along the line of sight (e.g., Doppler-boosted luminosity: Padovani & Urry 1990; apparent superluminal motion of VLBI radio components: Zensus 1989; and variability on timescales as short as minutes to hours: Heidt & Wagner 1996). Indeed, BL Lacs display some of the most extreme behavior of any class of AGN. Given their large X-ray luminosities BL Lacs are found in modestly large numbers in X-ray surveys (e.g., 43 in the *Einstein* Extended Medium Sensitivity Survey (EMSS): Stocke et al. 1991, Rector et al. 1999; 66 in the *Einstein* “Slew Survey”: Perlman et al. 1996b; and 120 in the ROSAT-Green Bank (RGB) Catalog: Laurent-Muehleisen et al. 1998). There may well be of order 1000 BL Lacs hidden among all the sources in the ROSAT All-Sky Survey (RASS; e.g., Nass et al. 1996; Bade et al. 1998).

Many observations (e.g., extended radio luminosity and morphology: Antonucci & Ulvestad 1985; Perlman & Stocke 1993; host galaxy luminosity and morphology: Abraham et al. 1991; Wurtz, Stocke & Yee 1996; comparative space densities and lu-

minosity functions: Padovani and Urry 1990, M91) suggest that BL Lac objects are relativistically-beamed “Fanaroff & Riley class 1” (FR-1) radio galaxies, which are low-luminosity, edge-darkened sources often found in rich and poor cluster environments. BL Lacs discovered by both X-ray-selection (XBLs) and radio-selection (RBLs) techniques share these characteristics, strongly suggesting that XBLs and RBLs are from the same parent population. And although XBLs and RBLs have somewhat different observed properties (e.g., XBLs have larger starlight and smaller polarized flux fractions optically: M91; Jannuzzi et al. 1993, 1994 and lower radio core dominance values: Perlman & Stocke 1993, Laurent-Muehleisen et al. 1993), most of these differences can be accommodated either by invoking different mean viewing angles, wherein XBLs are viewed further from their beaming axis (e.g., Stocke et al. 1989) or by invoking different electron energy distributions (Giommi & Padovani 1994). But many RBLs have extended radio and optical emission-line luminosities inconsistent with being FR-1s (Rector & Stocke 1999) and, most surprising, Stocke & Rector (1997) have found a large excess of MgII absorption systems in the 1Jy RBL sample, suggestive of gravitational lensing. Thus, while XBLs seem mostly consistent with being beamed FR-1s, RBLs seem to be a mixture of beamed FR-1s and FR-2s as well as a few gravitationally-lensed quasars.

Recent work on the clustering environments of BL Lacs by Wurtz et al. (1997) finds that BL Lacs avoid rich clusters and

¹Visiting Astronomer, Kitt Peak National Observatory, National Optical Astronomy Observatories, which is operated by the Association of Universities for Research in Astronomy, Inc. (AURA) under cooperative agreement with the National Science Foundation.

²Visiting Astronomer, Multiple Mirror Telescope Observatory. MMTO is owned and operated by the Smithsonian Astrophysical Observatory and the University of Arizona.

³Visiting Astronomer, National Radio Astronomy Observatory. NRAO is a facility of the National Science Foundation operated under cooperative agreement by Associated Universities, Inc.

⁴Current address: National Optical Astronomy Observatories, 950 N. Cherry Ave., Tucson, AZ 85719

the most luminous galaxies (i.e., the brightest cluster galaxies) at low redshifts, suggesting that there may be a problem with this simple picture. Also, Owen, Ledlow & Keel (1996) failed to find substantial numbers of BL Lac candidates among their large (~ 200) sample of rich cluster radio galaxies. Either there exists some physical reason why BL Lacs avoid rich clusters at low z or current surveys systematically miss BL Lacs in rich clusters (see Wurtz et al. 1997 for suggested reasons). Another observation that does not fit the simple beamed FR-1 picture is the disparity in $\langle V/V_{max} \rangle$ values for RBLs and XBLs (0.61 ± 0.05 for RBLs in the 1Jy survey; Rector & Stocke 1999; 0.33 ± 0.06 for XBLs in the EMSS; M91, Perlman et al. 1996b), which suggests that they may be from different populations and/or that one or both samples are incomplete. Indeed, Della Ceca (1993) first pointed out that raising the X-ray flux limit of the EMSS sample to $f_x \geq 10^{-12}$ ergs s^{-1} cm^{-2} raises $\langle V/V_{max} \rangle$ to 0.48 ± 0.06 , which is consistent with no evolution. Thus incompleteness of the EMSS sample at faint fluxes is a real concern.

Browne & Marchā (1993; hereafter BM93) and Marchā & Browne (1995; hereafter MB95) describe an effect which can make radio- and X-ray-selected BL Lacs difficult to recognize optically, thus introducing the possibility that such samples are incomplete: A BL Lac object at low redshift with a flux density near the survey limit (i.e., a “low-luminosity BL Lac”) would be difficult to identify optically because the weak nonthermal continuum from the AGN could be fainter than the starlight from the luminous host elliptical galaxy, thus causing these X-ray or radio sources to be misidentified as either “normal” elliptical galaxies or as clusters of galaxies rather than as BL Lacs. This effect (hereafter called the “B-M effect”) will result in a paucity of BL Lacs at low z , thus flattening the observed X-ray luminosity function (XLF) at the low-luminosity end (MB95). The $\langle V/V_{max} \rangle$ for the sample will also be artificially decreased, as this effect causes the flux limit of the sample to be underestimated. BM93 suggested that the EMSS BL Lac sample may be incomplete on the basis of the sample flux limit and the XLF. However, in a more detailed analysis MB95 find that, while there is some evidence for “hidden” BL Lacs, the XLF and $\langle V/V_{max} \rangle$ statistics of the EMSS sample cannot be altered significantly by this selection effect; and so it probably cannot explain the $\langle V/V_{max} \rangle$ discrepancy between the EMSS and 1Jy samples (MB95).

In this paper we present evidence for a small population of low-luminosity BL Lac objects that were originally misidentified as clusters of galaxies in the EMSS (§2). These objects were identified using ROSAT HRI observations which reveal the presence of point-like X-ray emission at the location of a low-power radio galaxy, thus revealing the presence of a weak AGN (§3). Subsequent optical spectroscopy and VLA imaging confirm that these sources are BL Lacs (§4). Individual sources are discussed in §5. Since the EMSS is the only statistically-complete X-ray-selected sample of BL Lacs for which the XLF and evolution have been calculated, these results affect the XLF and evolution determinations as well as physical models of BL Lacs (e.g., Ghisellini & Maraschi 1989). However, based upon the small number of new EMSS BL Lacs discovered, the modifications to earlier XLF evolution and $\langle V/V_{max} \rangle$ determinations are slight (§6).

2. THE SAMPLE SELECTED FOR ROSAT HRI OBSERVATION

The *Einstein* Medium Sensitivity Survey (EMSS; Gioia et al. 1990; Stocke et al. 1991; Maccacaro et al. 1994) contains

835 faint ($> 7 \times 10^{-14}$ ergs cm^{-2} s^{-1} in the $0.3 - 3.5$ keV soft X-ray band) X-ray sources discovered serendipitously with *Einstein* Imaging Proportional Counter (IPC) images obtained of various targets at high Galactic latitude ($b > 20^\circ$). To be included in the EMSS a source detection limit of 4σ above the X-ray plus detector backgrounds is imposed.

The full EMSS sample of BL Lac objects currently consists of 43 objects with X-ray fluxes from 10^{-11} to 10^{-13} ergs s^{-1} cm^{-2} in the $0.3-3.5$ keV band (Rector et al. 1999). The identification of these objects followed both a spectroscopic and a photometric set of criteria as outlined in Stocke et al. (1991), as did the identification of the other classes of X-ray sources identified in the EMSS (e.g., QSOs and Seyferts, clusters of galaxies, normal galaxies and Galactic stars).

Based upon the nearly complete identifications of sources in the EMSS survey, we assembled a list of the best candidates of potentially misidentified clusters of galaxies. In particular, we concentrated our efforts on the EMSS subsample from which the “complete” BL Lac sample of M91 was extracted. This sample of BL Lacs was selected by the following criteria: An X-ray flux of $f_x \geq 5.0 \times 10^{-13}$ ergs s^{-1} cm^{-2} and a declination limit of $\delta \geq -20^\circ$. The X-ray-selected objects drawn from the EMSS using these constraints are fully identified; thus incompleteness of the M91 BL Lac sample can only occur from the misidentification of sources. The sample selected for ROSAT HRI observations includes all suspect sources within the bounds of the M91 subsample plus the best cases for misidentified BL Lacs in the rest of the EMSS. Our criteria for what constitutes a suspect source are detailed below.

2.1. Candidates from the M91 Subsample

In compiling the suspect source list we eliminated very well-resolved X-ray sources whose extended flux so dominates over any possibly embedded point source that it would be below the flux limit of the EMSS. Many of the EMSS clusters have been studied with ROSAT, confirming their extended nature. So, using either ROSAT PSPC or HRI or the original *Einstein* IPC images, the maximum point source contribution to the IPC detect cell counts is measured by fitting a point source at the location of the the detected cluster radio galaxy or galaxies. Since most EMSS sources were detected quite close to the signal-to-noise limit (4σ), it was unlikely that any point source contribution to extended cluster emission would be detected on its own. But, it is important to note that, while these radio galaxies might be excluded from being EMSS BL Lacs, they still could be low-luminosity BL Lacs; i.e., the cluster is the correct X-ray identification, but a low-luminosity BL Lac is nevertheless present within the cluster. One such source (MS 0011.7+0837) was discovered in the course of this study.

X-ray clusters lacking radio sources were also eliminated from the suspect list, as radio-quiet BL Lacs are not believed to exist (Stocke et al. 1990). VLA surveys of EMSS clusters (Stocke et al. 1991, Stocke et al. 1999) have been conducted, which are deep enough to detect most FR-1 radio galaxies in a cluster. The VLA snapshot survey of all EMSS sources reported in Stocke et al. (1991) has a 5σ detection limit of ~ 1 mJy at 5 GHz, which should be sufficient to detect radio galaxies in nearby clusters (a detection limit of $\log L_r \geq 23$ W Hz^{-1} for $z \leq 0.2$). A deeper VLA survey has recently been completed at 1.4 GHz for all EMSS clusters with $z \geq 0.3$ (Stocke et al. 1999). These new observations were timed to achieve a point-source radio power limit of $\log L_r \geq 23.5$ W Hz^{-1} . While this limit is not quite deep enough to detect all FR-1s,

BL Lacs have Doppler-boosted cores which add significantly to the total radio power level of an FR-1. Thus, the combination of these two sets of radio observations should be adequate to detect all potential BL Lacs in EMSS clusters. Using the observed optical luminosities of BL Lac host galaxies from Wurtz, Stocke & Yee (1996), the power limits of the above mentioned VLA surveys require that any non-detection falls at $\alpha_{ro} \leq 0.2$, well below the level of BL Lacs (see Stocke et al. 1991 and Section 6 herein). Therefore, we have eliminated clusters from the suspect list if no radio sources were detected by these surveys.

Clusters with radio galaxies whose optical spectra are dominated by bright emission lines (i.e., “cooling flow” clusters) were originally eliminated from the suspect list due to the usual BL Lac classification criterion which requires “featureless” optical spectra (see below). However, the luminous, low-ionization optical emission lines found in the spectra of the brightest cluster galaxies (BCGs) in cooling flow clusters are very extended and not directly related to either the broad- or narrow-line regions of an AGN. Moreover, these clusters also contain central “cusps” in their X-ray surface brightness distributions, which could hide the presence of a low-luminosity point source associated with the BCG and these BCGs are often weak radio emitters. Thus, these BCGs are potential low-luminosity BL Lac objects if we ignore the optical line emission. So, although the presence of an X-ray point source is not the usual interpretation for the X-ray “cusps” in cooling flow clusters (e.g., Fabian 1994), we have scrutinized all the cooling flow clusters whose BCGs are radio galaxies to ensure that the excess central surface brightness could not hide a point source so luminous that a potential EMSS BL Lac could be present (see above). Eleven such clusters were scrutinized using archival ROSAT and/or Einstein data. All but four of these clusters are easily too extended to harbor a point source luminous enough to be a member of the EMSS sample. Two of these four (MS 0102.3+3255 & MS 1244.2+7114) are marginally resolved by current observations so that a BL Lac could be present. Another cooling flow cluster (MS 1455.0+2232) is very well-resolved by a pointed PSPC observation. But, because this source was detected at a very high significance level in the EMSS, an embedded point source of only $\sim 20\%$ of the IPC detect cell flux would still be an EMSS source. Since the cooling flow “cusp” in the PSPC image of this source could hide a point source which is $\sim 15\%$ of the detect cell flux, we must consider the BCG in MS 1455.0+2232 a possible low-luminosity BL Lac. The final source (MS 2348.0+2913) appears unresolved both in the ROSAT all-sky survey and in an off-axis PSPC pointing and so must be considered a likely BL Lac object. However, since we had not considered the possibility that “cooling flow clusters” could contain BL Lacs until this point was raised by the referee, we were unable to obtain ROSAT HRI images of these interesting sources.

No EMSS sources identified as “normal” galaxies meet the above criteria to be suspect; most normal galaxies have quite extended X-ray emission and only a few are radio emitters. We note that deep ROSAT HRI observations of normal galaxies from the EMSS catalog by ourselves and others (Dahlem & Stuhrmann 1998; Stocke, Rector & Griffiths 1999) do not find galaxies with strong, nuclear point sources. Any point sources present do not dominate the total X-ray flux; thus these objects were not detected as BL Lacs on the basis of their X-ray emission and so would not be included in the EMSS BL Lac sample.

A total of seven candidates for misidentification emerged from this selection process, all of which have been observed

by the ROSAT HRI (excepting the four cooling flow clusters identified as suspect only after the HRI observations were obtained). These are all of the sources in the EMSS subsample of M91 that meet the above criteria.

2.2. Other Low-Luminosity BL Lac Candidates & Classification Criteria

Because it is possible that low-luminosity BL Lacs may be present in the EMSS but not in the bright M91 complete subsample, we have also included five additional EMSS sources which meet the selection criteria to be suspect identifications but are below the flux or declination limits of the M91 sample. These five may not be all of the suspect sources in the EMSS sample which are outside the M91 subsample, but are just the best cases we have found to this date. All of these objects have been observed by the ROSAT HRI as well.

Besides these new HRI observations, the classification criteria previously used to classify an X-ray source as a BL Lac require both optical spectroscopy and radio imaging. Therefore, we obtained new optical and radio data to determine whether these new candidates meet these BL Lac criteria. But, because these new sources may stretch the boundaries of the BL Lac class, the previously used criteria may need modification. These criteria are (Stocke et al. 1991): (1) unresolved at X-ray wavelengths; (2) comparable to or more luminous than a typical FR-1 radio galaxy at radio wavelengths (e.g., $\log L_r \geq 23$ W Hz $^{-1}$). (3) “featureless” optical spectra in terms of emission lines (i.e., any emission line must be quite weak; i.e., $W_\lambda \leq 5\text{\AA}$); and (4) “featureless” optical spectra in terms of absorption lines (i.e., the presence of a nonthermal component to the optical continuum, as indicated by a CaII break “contrast” of $< 25\%$; which corresponds to $D(4000) \leq 1.33$ as defined in Dressler & Shectman 1987). The last two criteria are somewhat arbitrary as originally described by Stocke et al. (1991). Specifically, criterion #4 is violated by three objects herein which are otherwise BL Lac-like, as BM93 predicted. Further, Marchă et al. (1996) proposed a further relaxation of the criteria, which is discussed in §6. Also because some low-luminosity BL Lacs may be embedded in extended cluster X-ray emission, criterion #1 may need reevaluation as well. For sources observed with the VLA, an edge-darkened FR-1 extended radio luminosity and morphology surrounding a bright point source is expected but is not required for classifying the source as a BL Lac, since a few BL Lacs have FR-2 morphologies. Also implicit in the above criteria is that the X-ray and radio core positions must coincide. We note that optical polarization, often a criterion used for classification of BL Lacs, is not considered here primarily because polarimetry has not yet been obtained for these objects. However, polarimetry blue-ward of the CaII break would provide important confirmation that the present candidates are BL Lac objects.

A secondary set of photometric criteria were also used in Stocke et al. (1991) to cross-check potential identifications. Specifically for BL Lac objects, a broad-band color criterion is made possible by their unique spectral energy distributions. That is, XBLs are found to occupy a nearly unique area in the $(\alpha_{ro}, \alpha_{ox})$ plot (see §4), where these spectral indices refer to radio-to-optical and optical-to-X-ray respectively as defined in Stocke et al. (1991). This criterion was rigorously tested by using the *Einstein* Slew Survey data to predict BL Lac object identifications (Perlman et al. 1996a) and was found to be $> 90\%$ successful in predicting such identifications prior to optical spectroscopy. As with previously identified EMSS

BL Lacs, we will use this photometric criterion to check low-luminosity BL Lac candidates.

3. X-RAY OBSERVATIONS

Twelve BL Lac candidates were observed with the ROSAT HRI during AO1, AO5 and AO7. The log of ROSAT observations for our sample are listed in Table 1. Col. [1] is the EMSS object name. Cols. [2]-[4] list the ROSAT observation request (ROR) number, the date of the pointed observation, and the effective exposure time; Col [5] indicates whether or not the object meets the EMSS complete subsample criterion of M91 described above; and Cols [6] and [7] list the HRI position of the source; for extended sources the position marks the peak flux.

XIMAGE (v2.5; part of the XANADU⁵ package) and FTOOLS⁶ (v.4.0) were used to determine whether or not a source was resolved by matching the nominal on-axis Encircled Energy Function (EEF) of the HRI to the radial profile of each source. The EEF should be viewed as the HRI response function to a point source; however, other effects (e.g., pointing “jitter” and aspect solution errors; Morse 1994) may alter the actual point source response from the EEF. The radial profiles for the unresolved and resolved sources are shown in Figures 1 and 2 respectively. Radial profiles for MS 1317.0-2111 and MS 1520.1+3002 are not shown because no X-ray source was detected by the HRI at the position of the radio galaxy for either source. Six sources are unambiguously unresolved, one (MS 0011.7+0837) is marginally resolved and the remaining are well-resolved by these observations. Figure 1 shows that even the unresolved sources do not exactly match the EEF at a radius of $\leq 8''$, whereas 87% of the point-source flux should be within this radius. This is due to a halo in excess of the nominal EEF at a radius of $\sim 10''$. This “excess halo” has been noted in other HRI observational programs, including the calibration star HZ 43, but an explanation has not yet been found (D.E. Harris 1997, private communication). Since the “excess halo” is also consistently present in the point spread function of stars within the fields of our observations, we are confident that these sources are not resolved despite this $\sim 1\sigma$ excess over the nominal EEF. Contoured, grey-scale HRI maps of the resolved sources are shown in Figure 3.

Two sources (MS 0011.7+0837 and MS 1826.5+7256) did not exactly match the HRI EEF and it was questionable as to whether or not they were resolved. After further analysis of MS 0011.7+0837 we are confident that it is spatially resolved. To confirm that its extended flux was not due to misalignment of the individual observation intervals (“OBIs”) or jitter within each OBI, the following test was done on the nearby EMSS source MS 0011.6+0840, a bright K0 V star fortuitously within the field of the HRI and sufficiently “on axis” to have the same EEF (its offset from field center is 4.8'). The observation was split into the four different OBIs and the centroid for MS 0011.6+0840 was determined for each OBI. The OBIs were then restacked, with each OBI linearly shifted to align the centroids. MS 0011.7+0837 and MS 0011.6+0840 were then compared to the HRI EEF. The original stacking of OBIs suffered from minor misalignment, and there is some evidence for jitter within two of the four OBIs. However, the energy profile for MS 0011.6+0840 extracted from the restacked image matches the nominal HRI EEF quite well while the energy profile

for MS 0011.7+0837 does not (Figure 4); the probability that the energy profile of MS 0011.7+0837 is the same as MS 0011.6+0840 is $\sim 1\%$ (the variance summed over all the annuli is $\sigma = 3.77 \pm 0.27$). Further, MS 0011.7+0837 is significantly elongated along the E-W axis (see Figure 3). However, because MS 0011.7+0837 contains either a radio galaxy or low-luminosity BL Lac embedded in extended cluster emission, we have included it in the other tests of the unresolved sources for thoroughness (see below).

The HRI field for MS 1826.5+7256 also contains an unidentified star at $\alpha = 18^h 27^m 42.8^s$, $\delta = +72^\circ 54' 53.0''$ (B1950), which allowed us to perform the same analysis as above. The radial energy profiles for neither MS 1826.5+7256 nor the in-field star match the HRI EEF. However, the radial energy profile for MS 1826.5+7256 is completely consistent with that of the star; the probability that they are the same is $> 95\%$ ($\sigma = 0.01 \pm 0.34$). The cause of the poor fit of MS 1826.5+7256 and the star to the nominal HRI EEF is unknown, but the integration time for this source was significantly longer than for the other sources, so it may have been caused by excessive jitter (MS 1826.5+7256 was observed in AO1).

The HRI position of MS 1826.5+7256 coincides with the optical position of a faint M5 V star ($V \approx 17$) at $\alpha = 18^h 26^m 25.8^s$, $\delta = +72^\circ 56' 06.5''$ (B1950). So MS 1826.5+7256 is unresolved, but it is not a BL Lac. Note that the optical position of MS 1826.5+7256 given in Maccacaro et al. (1994) is in error; the optical position given is that of a K star $19''$ to the NE of the true optical identification at the position quoted above.

The fluxes of the unresolved sources were measured by using an aperture of $75''$ in radius to determine the source count rate. As can be seen in Figure 1 this radius is more than sufficient to enclose all the flux from the source. The background count rate was determined by using a $100''$ to $200''$ annulus around the source; the background was then subtracted from the source count rate. The HRI has essentially no spectral resolution so the counts are modeled using a power-law spectrum of the form $F_\nu \propto \nu^{-\alpha}$. The X-ray spectral index α was estimated using the luminosity vs. X-ray spectral index correlation from Padovani & Giommi (1996) for all but MS 1019.0+5139 and MS 1209.0+3917. The spectral index for these two sources was determined by ROSAT PSPC observations (Blair et al. 1997). The flux was corrected for neutral Hydrogen absorption, assuming the Morrison & McCammon (1983) absorption model and neutral hydrogen column densities along the line of sight obtained from Gioia et al. (1990). Table 2 contains the X-ray properties of the unresolved sources (excluding MS 1826.5+7256, which is discussed above) and MS 0011.7+0837, including by column: [1] EMSS source name; [2] whether or not it is a member of the complete sample of M91; [3] the logarithmic density of galactic neutral Hydrogen toward the source (cm^{-2} ; Gioia et al. 1990); [4] the soft X-ray power-law energy spectral index; [5] the ROSAT HRI flux ($0.1 - 2.4$ keV) in units of $10^{-13} \text{ erg s}^{-1} \text{ cm}^{-2}$, corrected for the n_H in column 2 and assuming the spectral index in column 4; [6] is the logarithmic HRI luminosity in erg s^{-1} assuming $H_0 = 50 \text{ km s}^{-1} \text{ Mpc}^{-1}$, $q_0 = 0$; [7] the observed EMSS IPC flux ($0.3 - 3.5$ keV) in units of $10^{-13} \text{ erg s}^{-1} \text{ cm}^{-2}$, corrected for n_H absorption and assuming a spectral index of $\alpha_x = 1$ (Gioia et al. (1990)); [8] is the same as column [7] except assuming α_x from column [4];

⁵XANADU is provided by LHEA/NASA.

⁶FTOOLS is provided by LHEA/NASA.

Column [7] is the best estimate of the IPC flux if the source is dominated by extended cluster emission, column [8] is the best estimate if the source is dominated by a BL Lac object; and [9] is the fraction of predicted to observed IPC flux (see description below).

It is possible that faint, very extended structure from an associated cluster may be present around some of the unresolved sources. This extended emission may have been detected by the low-resolution *Einstein* IPC but was undetected by the higher-resolution ROSAT HRI due to a lower signal-to-noise ratio per pixel for the HRI. To determine whether or not there was any “missing flux” in the HRI observations we converted the HRI flux to an “expected” IPC flux by accounting for the different bands of the ROSAT HRI (0.1 - 2.4 keV) and the *Einstein* IPC (0.3 - 3.5 keV). We assume the X-ray spectral index α_x for the BL Lac to be valid across the *Einstein* IPC band, which is reasonable because the HRI and IPC bands significantly overlap. The HRI flux measurements are comparable (i.e., within 50%) to the IPC flux for three of the five BL Lac candidates. The exceptions, MS 1019.0+5139 and MS 1205.7-2921, are approximately three times brighter than measured by the IPC. Allowing for the variability of BL Lac X-ray emission (factors of $\sim 2-3$ are typical; e.g., Sambruna et al. 1995) we conclude that the HRI flux levels for the five BL Lac candidates are consistent with the *Einstein* IPC flux being entirely from an unresolved BL Lac X-ray emitter and that significant amounts of extended diffuse flux are not present. On the other hand, the total detected HRI flux for MS 0011.7+0837 is only 17% of the IPC flux. While it may be possible that this source is a BL Lac that was observed by the IPC in a flaring state, it is much more likely that the HRI has simply missed faint extended flux associated with a cluster because it is marginally resolved by the HRI. The optical and radio data (see below) also support the conclusion that the X-ray source MS 0011.7+0837 is not simply a BL Lac object but either a radio galaxy or low-luminosity BL Lac embedded in diffuse cluster emission. Even if MS 0011.7+0837 is a combination of cluster and BL Lac X-ray emission, the analysis shown in Table 2 shows that any X-ray point source present likely contributes only a small fraction to the IPC detection.

The HRI maps for three sources, MS 0011.7+0837, MS 1004.2+1238 and MS 2301.3+1506, do not rule out the possibility of a small but significant (20-50%) contribution to the total X-ray flux by a BL Lac object embedded within the cluster. We note that these objects are *not* excluded from consideration as BL Lacs simply because they are resolved, but because these sources would not meet the EMSS 4σ detection criterion without the extended X-ray flux. In fact, no clusters in the EMSS are sufficiently bright such that an embedded BL Lac with $< 20\%$ of the total X-ray flux could be detected without the associated cluster emission (see §2.1).

4. OPTICAL AND RADIO OBSERVATIONS

Optical spectra of the radio galaxy in MS 0011.7+0837 and the BL Lac candidates MS 1050.7+4946 and MS 1154.1+4255 were obtained at the KPNO 2.1m telescope. A spectrum of the BL Lac candidate MS 1019.0+5139 was obtained at the Multiple Mirror Telescope Observatory (MMTO). Low-resolution gratings were used to obtain one full spectral order (4000Å - 8000Å) at $\sim 5\text{\AA}$ resolution. These spectra were extracted and analyzed in IRAF and flux calibration was performed using observations of flux standards at similar airmass. No correction was made for the loss of light at the slit; thus the derived fluxes are probably uncertain by a factor of ~ 2 . In the 2.1m

spectra the flux calibration redward of 6500Å is corrupted due to second-order overlap and should not be trusted. Also, the slit was not rotated to the parallactic angle, and so it is possible that the spectral shape and therefore the measurement of $D(4000)$ could be slightly affected. Archival spectra from the original EMSS identification program for the unresolved X-ray sources MS 1209.0+3917 and MS 1205.7-2921, taken at the Canada-France-Hawaii Telescope (CFHT) by Isabella Gioia and at the Las Campanas 100” by Simon Morris respectively, were also analyzed. The spectra of MS 1205.7-2921 and of MS 1209.0+3917 are not of high quality; higher SNR spectra should be obtained in order to determine more accurate values for $D(4000)$ and better emission line limits. These spectra are shown in Figure 5.

The spectra were used to determine whether or not the object met the BL Lac classification criteria (see §1) and to determine an accurate redshift. The redshift of the host galaxy for each object was determined by cross correlating the object spectrum with the giant elliptical galaxy NGC 3245 (as described in Ellingson & Yee 1994); the technique has an accuracy of ± 0.001 . We note that the redshift reported here for MS 1205.7-2921 ($z = 0.249$) is different than previously reported in Maccacaro et al. (1994). The CaII break $D(4000)$ value was determined by measuring the continuum flux level on either side of the CaII break (see Dressler & Shectman 1987 for the complete formalism). The typical $D(4000)$ for a normal cluster elliptical or S0 galaxy is ≈ 2.0 . Weak emission lines were detected in two objects, MS 1019.0+5139 and MS 1050.7+4946; the latter object has H α only marginally detected. For the other objects upper limits on the presence of emission lines for [O II], H β , [O III] and H α (if within the observed band) were calculated. The poorest limit for these lines is listed in Table 3. Interestingly only two other BL Lacs (MS 1235.4+6315 and MS 2316.3-4222) in the EMSS sample show any emission line features, and these are both quite weak [O II] emission lines. In contrast, a large fraction of radio-selected BL Lacs in the 1Jy sample (Stickel et al. 1991) possess weak but luminous emission lines in their spectra (Stickel, Fried & Kühr 1993; Rector & Stocke 1999). Figure 6 shows the location of these new BL Lacs in the diagnostic plot of Stocke et al. (1991).

Deep VLA continuum maps were taken for two sources which meet the selection criteria of the M91 complete sample (MS 1019.0+5139 and MS 1050.7+4946; see Figure 7 for a map of the latter) on 27 April 1997. We chose to observe with the B-array at 20cm with a 50MHz bandwidth to maximize sensitivity to extended, steep-spectrum structure while achieving $\sim 4''$ resolution, which is ideally suited for these nearby sources. Eight 10-minute scans, each bracketed by a 90-second scan on a primary VLA phase calibrator, yielded $\sim 150,000$ “visibilities” for each source. Scans were widely spaced to optimize (u, v) coverage; achieving a $0.02 \text{ mJy beam}^{-1}$ (1σ RMS) noise level. Additionally a 20cm A-array “snapshot” was taken of MS 0011.7+0837 (also shown in Figure 7), which has a 1σ noise level of $0.24 \text{ mJy beam}^{-1}$.

The data were reduced in a standard manner with the NRAO AIPS software package. The core flux was determined by fitting a point source to the core. The extended flux is the total flux, as determined by the region around the source containing all the extended structure, minus the core flux. The standard K and bandpass corrections are applied to the luminosity calculations: a power-law continuum of the form $F_\nu \propto \nu^{+\alpha}$ is assumed where $\alpha = -0.8$ for extended flux and $\alpha = +0.3$ for the core (values typical of BL Lacs; Perlman & Stocke 1993;

Stickel et al. 1991). We note that Perlman & Stocke (1993) instead use $\alpha = -0.3$ for the core (a value more typical of FR-1s). However, the effect of this discrepancy is slight because EMSS BL Lacs are typically at low redshift ($z \approx 0.3$). Perlman & Stocke (1993) describe additional cosmological distance effects which can bias the measured core and extended fluxes, particularly so in FR-1 sources at high redshift ($z > 0.2$). Corrections for these biases are not applied because they are not significant at the redshifts of MS 0011.7+0837 and MS 1050.7+4946 and are strongly source dependent.

The morphologies of MS 0011.7+0837 and MS 1050.7+4946 (shown in Figure 7) are typical of low-power FR-1 sources excepting that MS 1050.7+4946 is somewhat more core dominated than a typical FR-1. Its core dominance is comparable to other EMSS BL Lacs; however, based upon the VLA configuration used and its low z it is possible that not all the extended flux was detected. Thus the extended flux and core dominance values reported in Table 3 should be considered as upper limits.

Given its modest redshift of $z = 0.141$ it is unusual that no extended flux was detected for MS 1019.0+5139. We quote a very conservative upper limit on the extended flux in this source, which assumes an intrinsically large source (100 x 30 kpc²) with an extended surface brightness just below the noise level per beam; however this limit is still very low for an FR-1 and is lower than any other BL Lac in the EMSS sample (Rechter et al. 1999). MS 1019.0+5139 was detected by both the Faint Images of the Radio Sky at Twenty Centimeters (FIRST; B-array at 20cm; White et al. 1997) and the NRAO VLA Sky Survey (NVSS; D-array at 20cm; Condon et al. 1998) surveys but was not resolved in either. Interestingly, the flux of this source in the FIRST survey catalog is 3.3 mJy, nearly identical to the flux measured in our map; however the NVSS flux is significantly higher (5.1 ± 0.5 mJy), suggesting that extended flux may have been detected on larger scales; although variability is also a possible explanation. A high dynamic-range C-configuration 20cm map should be made of this source to determine whether or not it has significant extended flux.

The optical and radio properties of the unresolved sources are given in Table 3. Columns include: [1] EMSS source name; [2] redshift; [3] the V-band magnitude (Stocke et al. 1991); [4] the equivalent width of the strongest emission feature (or the largest 3σ upper limit if none are present) [5] the CaII break value $D(4000)$, as defined in Dressler & Shectman (1987); [6] and [7] the VLA core and total radio flux at 20cm (mJy), except where noted; [8] the core dominance, defined as the core to extended flux ratio; and [9] and [10] the VLA 20cm core and extended luminosities in $W\text{ Hz}^{-1}$.

The optical spectra for the newly discovered EMSS BL Lacs are shown in Figure 5. The spectrum for a typical EMSS BL Lac can be described as that of a luminous elliptical galaxy with a significant nonthermal component blueward of the CaII H&K break (rest $\lambda \approx 4000\text{\AA}$). It should be clear from Figure 5 that starlight from the host elliptical dominates the nonthermal continuum from the BL Lac in the V-band ($\sim 5500\text{\AA}$). Since, in these cases the X-ray and radio flux is dominated by the BL Lac but the optical flux is dominated by the host galaxy, the $(\alpha_{ox}, \alpha_{ro})$ values do not accurately reflect the properties of the BL Lacs themselves. To correct for this effect we determined the optical flux for each BL Lac by the following method: The host elliptical is assumed to have a CaII break strength of 50% (i.e., $D(4000) = 2.0$). Flux in excess of this amount blueward of the CaII break is assumed to be from the BL Lac itself. This flux is extrapolated to 5500\AA by using the spectral slope mea-

sured directly blueward of the break, if possible. If the spectrum is insufficient to determine the slope an optical spectral index of $\alpha_o = 1.0$ is assumed (Stocke et al. 1991). All of the BL Lacs in the EMSS sample with a significant elliptical component in their spectrum (i.e., $D(4000) > 1.0$) are corrected in this manner in Figure 8. Since this correction removes optical flux, the $(\alpha_{ox}, \alpha_{ro})$ values for the BL Lacs are displaced upwards and to the left. We note that we do not correct the measured equivalent width of emission lines for the presence of the host galaxy. As pointed out by Marcha et al. (1996), quite strong emission lines ($W_\lambda \leq 50\text{\AA}$ relative to the AGN alone) could be present without exceeding the traditional BL Lac criterion ($W_\lambda \leq 5\text{\AA}$ relative to the AGN *plus* host galaxy continuum).

We specifically note that MS 1019.0+5139 has a position in Figure 8 ($\alpha_{ox} = 0.72$; $\alpha_{ro} = 0.41$) fully consistent with a BL Lac object and not with a radio-quiet QSO or Seyfert galaxy. We are concerned about the nature of this particular object because it is the only EMSS BL Lac that possesses weak optical emission lines, a flat X-ray spectral slope and an unresolved radio source. Although Seyferts have much stronger emission lines, the other two attributes of MS 1019.0+5139 are more characteristic of Seyferts than BL Lacs. However the radio core power is much more characteristic of a radio galaxy than of a Seyfert. This potential transitional object deserves further observational attention.

5. DISCUSSION OF INDIVIDUAL SOURCES

MS 0011.7+0837 is marginally resolved by the ROSAT HRI. The peak of the X-ray emission coincides with the core of a radio galaxy, but the X-ray emission is elongated along the E-W axis (Figure 3). The maximum point source contribution to the X-ray emission at the position of the radio galaxy is $\sim 50\%$ of the observed ROSAT HRI flux (see Figure 4); however this is $< 8\%$ of the flux detected by the *Einstein* IPC (see discussion in §2). Thus this source was detected by the IPC because of the extended cluster emission, not because of the radio galaxy. The VLA A-array snapshot shows a classic FR-1 morphology (Figure 7) with a very low core dominance value, typical of a normal FR-1 radio galaxy. The optical identification is a prominent cD radio galaxy in a poor cluster at $\alpha = 00^h11^m45.5^s$, $\delta = +08^\circ37'19.4''$ (B1950) in the image of Gioia & Luppino (1994). The radio galaxy is the marked object in the finding chart for this source (Maccacaro et al. 1994). However, the Ca II break indicates the presence of a non-thermal continuum very similar to the other low-luminosity BL Lacs identified in this paper. The above evidence suggests that MS 0011.7+0837 is a normal radio galaxy or possibly a low-luminosity BL Lac within an X-ray cluster; however it is the cluster that is responsible for the IPC detection (see §3). The X-ray source $4.8'$ to the NW in Figure 3 is MS 0011.6+0840, the bright K0 V star used in the point-source analysis of MS 0011.7+0837. [ID = CLUSTER]

MS 0433.9+0957 is well resolved by the ROSAT HRI. Although the X-ray emission encompasses two radio galaxies, no distinct point sources are detected at their locations; any contribution of X-ray flux from point-sources at their positions is negligible. We identify this source as a cluster, in agreement with the optical identification of a loose, poor cluster in Gioia & Luppino (1994); one radio galaxy is located at the center of their image, and the second is $30''$ south and $20''$ east of center. [ID = CLUSTER]

MS 1004.2+1238 is well resolved by the ROSAT HRI. The optical field contains a loose cluster dominated by a central

radio-emitting galaxy (Stocke et. al. 1991). The radio and optical positions of the central galaxy do not match the HRI position; the HRI position of the peak flux is $\sim 9''$ to the north of the radio position (Figure 3). The maximum contribution of a point source at the location of the radio galaxy is $\sim 20\%$ the total X-ray flux. No X-ray flux is detected at the position of another radio galaxy $\sim 3'$ north of the cluster. The ROSAT HRI and *Einstein* IPC fluxes match only to within 50%, indicative of extended flux undetected by the HRI. The radio galaxy is the east of the two nuclei at the position marked by Maccacaro et al. (1994) in their finding chart. The optical spectrum of the radio galaxy has a strong CaII break ($D(4000) = 1.9$) and strong [O II] emission ($W_\lambda = 40\text{\AA}$), further suggesting it is not a BL Lac. [ID = CLUSTER]

MS 1019.0+5139 is unresolved by the ROSAT HRI. A deep B-array 20cm VLA map does not detect any extended structure above the 0.02 mJy beam $^{-1}$ noise level. Assuming a morphology and physical extent typical of XBLs (~ 100 kpc; Perlman & Stocke 1993) places a very low limit of $\log L_r < 22.67$ on its extended radio luminosity. The absence of extended flux to such a low-luminosity level is unusual for XBLs and is also rare among RBLs. Given its low redshift, a deep C-array 1.4 GHz mapping should be done to look for very diffuse extended structure. The radio core position matches the HRI position on the object marked in the finder of Maccacaro et al (1994). H α and [NII] 6549,6583 \AA are detected in emission in this object at the same redshift as the host galaxy; the W_λ for these lines are within the BL Lac classification limits. Its CaII break strength $D(4000) = 1.30$ (a “contrast” of 23%) is also consistent with the BL Lac selection criteria of Stocke et al. (1991). [ID = BL LAC]

MS 1050.7+4946 is unresolved by the ROSAT HRI. The B-array 20cm VLA map shows a classic FR-1 morphology but with a core to extended flux ratio quite large for a typical FR-1 (see Figure 7 and Table 3). The optical field shows a central dominant radio galaxy (marked in the finder chart of Maccacaro et al. 1994) in a very sparse cluster typical for BL Lacs (Wurtz et al. 1997). The radio position matches the HRI position. The optical spectrum shows possible weak ($W_\lambda = 2.5\text{\AA}$) H α in emission. Its CaII break strength $D(4000) = 1.47$ (a “contrast” of 32%) is somewhat strong for the selection criteria of Stocke et al. (1991), but it is not inconsistent with the relaxed criteria proposed by March \tilde{a} et al. (1996; see below); further, its X-ray and radio properties are more consistent with a BL Lac than a normal FR-1 radio galaxy. [ID = BL LAC]

MS 1154.1+4255 is unresolved by the ROSAT HRI. It also has the lowest X-ray luminosity amongst the EMSS BL Lacs. The radio position matches the HRI position. The optical field shows only a very sparse group of galaxies, with the BL Lac marked in the finder of Maccacaro et al. (1994). Like MS 1050.7+4946, its CaII break strength $D(4000) = 1.5$ (a “contrast” of 33%) is somewhat stronger than allowed by the selection criteria; it appears transitional from BL Lacs to the population of normal radio galaxies. The only available 20cm radio map for this source is from the FIRST survey (White et al. 1997), where it is unresolved; it is also unresolved in a VLA 6cm C-array snapshot (Gioia & Luppino 1994). [ID = BL LAC]

MS 1205.7-2921 is unresolved by the ROSAT HRI at the optical and radio position. This source was previously assigned a redshift of $z = 0.171$ based upon a tentative identification of Ca H&K (Stocke et al. 1991). The correct redshift is $z = 0.249$ based upon the detection of a relatively strong CaII

break ($D(4000) \approx 1.6$) and G-band at this redshift (see Figure 5). The strength of the CaII break is questioned due to the low quality of the available spectrum. Otherwise this object is mostly consistent with the BL Lac classification. The finding chart in Maccacaro et al (1994) identifies this BL Lac. [ID = BL LAC]

MS 1209.0+3917 is unresolved by the ROSAT HRI at the optical and radio position. This object was originally identified as a “cooling flow galaxy” (Stocke et al. 1991) based upon a poor optical spectrum, but it unambiguously meets the BL Lac classification criteria based upon the new optical spectrum shown in Figure 5. The only available 20cm radio map for this source is from the FIRST survey (White et al. 1997), where it is unresolved; it is also unresolved in a VLA 6cm C-array snapshot (Gioia & Luppino 1994). The radio position matches the HRI position on the object marked in the finder chart of Maccacaro et al. (1994). In the Gioia & Luppino (1994) image the BL Lac is at an approximate offset of $35''$ south and $17''$ east. [ID = BL LAC]

MS 1317.0-2111 is undetected by the ROSAT HRI. No sources are detected *at all* within the HRI field of view. A 3σ point-source detection limit at the position of the optical identification or the position of the blank-field radio source indicates its HRI flux is $f_x \leq 1.2 \times 10^{-13} \text{ erg cm}^{-2} \text{ s}^{-1}$. Converted to the IPC band assuming $\alpha_x = -1$ the upper limit on the flux is less than 30% of that measured by the *Einstein* IPC. No extended flux was detected within the IPC error circle; but we cannot exclude the possibility that the IPC source is very extended. The absence of an HRI detection is also consistent with a highly variable point source such as a BL Lac. It is also possible that this source is spurious. A deeper X-ray image is necessary to determine the nature of this source. [ID = UNKNOWN]

MS 1333.3+1725 was on our original observing list but was instead targeted by M. Hattori. Hattori & Morikawa (1998, private communication) report that this X-ray source is point-like at the position of an elliptical galaxy with a depressed Ca II break (I.M. Gioia 1998, private communication). Therefore, this source is a BL Lac object, not a cluster as originally reported by Stocke et al. (1991). Because it is not a member of the M91 complete sample and because we have not had the opportunity to scrutinize the X-ray data in the manner herein, this source will be discussed at a later time (Rector et al. 1999).

MS 1520.1+3002 is undetected by the ROSAT HRI at the position of the original optical identification. However, very extended X-ray emission is marginally detected coincident with a bright elliptical galaxy $\sim 30''$ south of the IPC error circle in Maccacaro et al. (1994). A weak ($f_x \approx 5 \times 10^{-14} \text{ erg cm}^{-2} \text{ s}^{-1}$), resolved X-ray source at $\alpha = 15^h 20^m 11.4^s$, $\delta = +30^\circ 05' 38.3''$ (B1950) is also marginally detected $2'$ north of the original optical identification, which may have caused the measured IPC position to be moved north. The nature of this source is unknown. While no optical spectrum was taken of the bright elliptical galaxy to the south, it is likely at the same redshift as members of the loose cluster within the field at $z = 0.117$. [ID = CLUSTER]

MS 1826.5+7256 is unresolved by the ROSAT HRI. This object does not match the EEF as well as the other unresolved sources but it does match the EEF extracted from an in-field star (Figure 4). This circumstance is most likely due to jitter during the long integration time. The HRI source position coincides with the optical position of an M5 V star. The optical field shows only two galaxies in the vicinity (Stocke et al. 1991), further supporting it is not a cluster. The marked object in the find-

ing chart of Maccacaro et al. (1994) is *not* the correct identification; the M5 V star at $\alpha = 18^h 26^m 25.8^s$, $\delta = +72^\circ 56' 06.5''$ (B1950) is the X-ray source, $\approx 20''$ southwest of the marked object. [ID = STAR]

MS 2301.3+1506 is well resolved by the ROSAT HRI. We identify it as a cluster, in agreement with the optical identification of a rich cluster with a dominant cD galaxy by Gioia & Luppino (1994). The peak of the X-ray flux coincides with the optical and radio position of a radio galaxy (Figure 3); however the maximum contribution of a point source at the location of the radio galaxy is $\sim 20\%$ of the total X-ray flux; thus the extended X-ray flux dominates over any point source present. The radio galaxy is centered in the image of Gioia & Luppino (1994) and is the marked object in the finding chart of Maccacaro et al. (1994). A possibly unresolved X-ray source is also detected $4.3'$ to the SW at $\alpha = 23^h 01^m 03.1^s$, $\delta = +15^\circ 04' 04.8''$ (B1950), which is well outside of the IPC error circle for MS 2301.3+1506 and does not contribute to the X-ray emission detected by the IPC for this source. This SW source was excluded from the EMSS because it was only a 2.8σ IPC detection; however, its HRI flux is rather bright ($f_x = 6.6 \times 10^{-13}$ erg s $^{-1}$ cm $^{-2}$), suggesting strong variability. It is in the field of view of the *R*-band image of MS 2301.3+1506 taken by Gioia & Luppino (1994); and its optical position matches a potential cluster member. Spectroscopy of this galaxy should be obtained to determine the nature of this source. [ID = CLUSTER]

6. RESULTS AND DISCUSSION

Six of the twelve X-ray sources observed by the ROSAT HRI are unresolved at $\sim 3''$ resolution: five are identified as BL Lac objects and one is identified as a M5 V star (MS 1826.5+7256). Since only 5 of the best 12 cases for identifications are actually BL Lacs, we have now identified the large majority of the EMSS BL Lacs, particularly in the well-scrutinized M91 complete sample. Thus, while some BL Lacs were originally misidentified in the EMSS, there are few such cases. And while there may still be a few BL Lacs embedded in “cooling flow” clusters that have not been thoroughly scrutinized using high resolution X-ray imaging, they are few in number and do not alter substantially the conclusions we draw in this Section.

The optical spectra of these new BL Lacs are “featureless,” in the sense of possessing no or only very weak emission lines. However, the CaII break in some of these sources is slightly stronger than in other XBLs (see Figure 6), as specifically predicted by BM93. MS 1050.7+4946, MS 1154.1+4255, MS 1205.7-2921 and MS 2306.1-2236 are examples of low- z objects which match the BL Lac classification except for their slightly stronger CaII break strengths, pushing the limits of the selection criteria of Stocke et al. (1991). Their CaII break strengths are located “in the gap” between BL Lacs and FR-1 radio galaxies (see Figure 6), suggesting a smooth transition between the two populations. The value of the CaII break strength criterion of 25% ($D(4000) \leq 1.33$) suggested by Stocke et al. (1991) is somewhat arbitrary. Marchā et al. (1996) note that nearly all ($> 95\%$) galaxies with a CaII break strength $\leq 40\%$ ($D(4000) \leq 1.67$) must have an extra source of optical continuum. These objects otherwise have BL Lac-like characteristics including luminous point X-ray emission and low-power, core-dominated radio sources. Thus, we feel confident in classifying them as BL Lac objects.

The broadband spectral energy distributions (α_{ox}, α_{ro}) for the new BL Lac objects, once corrected for the presence of the luminous host elliptical galaxy as described in §4, are similar

to the other BL Lacs in the EMSS. Thus, as with the other EMSS BL Lac objects, the photometric classification scheme of Stocke et al. (1991) confirms these objects to be BL Lacs.

Owen, Ledlow & Keel (1996) discovered four FR-1 radio galaxies which they describe as potential “weak” BL Lac objects because they are BL Lac-like, with no strong optical emission lines and a nonthermal origin of the depressed CaII break. These four objects do meet our relaxed CaII criteria but two of them, 3C 264 and IC 310, show H α +[N II] emission lines whose W_λ slightly exceed the BL Lac criterion. However, we note that the W_λ of these lines would be below the criterion limit if the nonthermal optical continuum in these objects were increased only slightly such that $D(4000) \leq 1.33$. These objects do meet the relaxed $W_\lambda, D(4000)$ criteria proposed by Marchā et al. (1996; see Figure 6). Like MS 1019.0+5139, the strength of the H α +[N II] emission lines in 3C 264 and IC 310 are comparable to FR-1s ($\log L \approx 40$ erg s $^{-1}$).

Owen, Ledlow & Keel (1996) argue against a BL Lac identification for these four objects because they are lobe-dominated radio sources ($f_{core} < f_{ext}$). While this is unusual for BL Lacs, it is consistent with being a source that is not highly beamed. The relationship of these objects to the low-luminosity BL Lacs discovered here is not yet known, although they are similar in many ways. ROSAT PSPC observations are available for two of these four weak BL Lac candidates (3C 264 in Abell 1367; Prieto 1996 and IC 310 in The Perseus Cluster; Rhee et al. 1994). Both of these AGN have apparent point-source detections which coincide with the radio core, strongly suggestive that they are low-luminosity BL Lac objects. 3C 264 and IC 310 have been placed in the $(\alpha_{ro}, \alpha_{ox})$ plot in Figure 8 by estimating the point-source X-ray fluxes and by correcting the optical flux for the presence of the host elliptical. Their location in the BL Lac area confirms our inference that these objects are weak BL Lacs. ROSAT HRI point-source detections at the location of the other two radio galaxies (1005+006 and 1442+195) would confirm these to be BL Lac objects as well as provide confirmation of an important new method for finding low-luminosity BL Lacs. We note that 3C 264 is a member of the 1Jy catalog (Kühr et al. 1981); thus, if it is indeed a BL Lac the 1Jy sample of BL Lacs (Stickel et al. 1991) is incomplete (MB95). We investigate this issue further in another paper (Rector & Stocke 1999).

Of the five newly discovered EMSS BL Lacs only two are in the complete M91 sample. The X-ray luminosities of these two new BL Lacs are the two lowest in the M91 sample, with an average luminosity ($\log \langle L_x \rangle = 44.10$) somewhat lower than the other BL Lacs in the M91 sample ($\log \langle L_x \rangle = 45.32$). A *t*-test shows the difference in luminosity distributions to be significant (probability $> 99\%$); so a few low-luminosity BL Lacs were systematically misclassified as clusters of galaxies in the original accounting of the EMSS.

Are these the “low-luminosity” BL Lacs predicted by BM93? BM93 estimate that the probability of correctly identifying a BL Lac with a flux near the sample limit drops dramatically with decreasing redshift because the weak nonthermal continuum from the AGN will be dominated by the host galaxy starlight. Optically this object’s spectrum could have too strong a CaII break to be classified as a BL Lac using the criterion suggested by Stocke et al. (1991). Based upon this optical classification criterion BM93 estimate that a BL Lac in the EMSS sample at $z < 0.2$ would have a probability of less than 30% (and those at $z < 0.1$ have less than 5%) of being correctly identified as BL Lacs in the EMSS survey. Thus, it is not sur-

prising that both of the newly identified BL Lacs in the M91 sample are at a $z \sim 0.2$ and have CaII breaks which slightly exceed the BL Lac criterion. However, in their analysis BM93 assume an X-ray flux limit for the EMSS sample of $S_x = 10^{-8}$ Jy ($f_x = 7.7 \times 10^{-14}$ ergs s^{-1} cm^{-2} for the IPC band), which is more than six times fainter than the cutoff for the the complete M91 sample. Due to its bright flux limit the M91 complete sample is relatively immune to the problem of misidentification described in BM93. MB95 estimate that 25% of the full EMSS cluster sample (5 or 6 objects) were misidentified; therefore it is not surprising that we have discovered only two instances of misidentification in the M91 sample. An analysis of a complete X-ray sample with a much fainter flux limit ($S_x \leq 10^{-8}$ Jy) is necessary to confirm the BM93 hypothesis. Such an analysis is in progress using the fainter sources in the EMSS (Rector et al. 1999).

Because of its moderate sensitivity and substantial sky coverage the EMSS is a suitable survey for discovering low-luminosity BL Lacs. These new objects allow the XBL X-ray luminosity function (XLF) to be extended to slightly lower energies ($44.0 < \log L_x < 44.3$). The number of objects discovered at these lower energies (two: MS 1019.0+5139 and MS 1050.7+4946) is consistent with an extrapolation of the previous XLF derived in M91; that is, we do not measure any significant steepening or flattening of the XLF to lower luminosities ($\log L_x \leq 44.3$) than the previously published XLF in M91. Including these two new low-luminosity BL Lac objects slightly raises the $\langle V/V_{max} \rangle$ value for the M91 XBL sample to 0.399 ± 0.06 . Since the latest value for the 1Jy radio-selected BL Lac sample is $\langle V/V_{max} \rangle = 0.614 \pm 0.05$ (Rector & Stocke 1999), these newly discovered BL Lacs do not ameliorate the discrepancy between XBLs and RBLs. Therefore, the possibility that these two selection techniques are sensitive to finding different types of BL Lacs must still be considered.

Because the EMSS is a “serendipitous” survey, it is possible the M91 sample may have been biased against previously known low- z , bright BL Lacs which were targets of IPC observations. However, the number of such objects in the 835 deg^2 sky coverage of the EMSS is likely quite small, ~ 1 object based upon known space densities (M91, Perlman et al. 1996a). A recent sample selected by the RASS (Bade et al. 1998) confirms this effect as it finds three BL Lacs at $z < 0.1$ in a sky area roughly three times that surveyed by the EMSS; two of these BL Lacs (Mkn 180 and I Zw 187) were previously known. If either of these two objects were included in the EMSS, the $\langle V/V_{max} \rangle$ would slightly decrease due to their high flux. Therefore, the XBL/RBL $\langle V/V_{max} \rangle$ discrepancy remains despite this selection bias in the EMSS. Further, the new RASS XBL samples of Bade et al. (1998) and Giommi, Menna & Padovani (1998) confirm the negative evolution of XBLs.

A discussion of the impact of these observations on the cluster X-ray luminosity function will be included in a future publication (Lewis, Stocke, Ellingson & Gioia 1999).

7. CONCLUSIONS

We have used the ROSAT HRI to search for BL Lac objects originally misidentified as galaxies or clusters of galaxies within the EMSS sample. Five new BL Lacs have been identified by this process, two of which are new members of the M91 complete subsample. Therefore, such misidentifications do not significantly affect the completeness of the BL Lac sample of M91. Because only two of the seven potential M91 subsample objects were found to be BL Lacs (and only 5 of 12 overall);

and because these 12 were reobserved with the ROSAT HRI as the most likely misidentifications we expect that there are very few remaining misidentified sources in the EMSS. It is also unlikely that many more low-luminosity BL Lacs will be discovered within the EMSS as nearly all the potential candidates have been investigated. Thus we believe that contamination of the EMSS sample from misidentification is not significant.

While it was the intention of this observing program to obtain ROSAT HRI images of all suspect X-ray sources in the M91 subsample, we had not considered the possibility (raised by the referee) that “cooling flow” clusters might hide point X-ray sources in their central surface brightness “cusps.” We had not made this consideration heretofore because this is not the usual interpretation of these cusps (Fabian 1994) and because the BCGs/radio galaxies in these clusters contain luminous emission lines in their optical spectra which easily exceed the equivalent width limits proposed for BL Lacs in Stocke et al. (1991). However, these luminous, low ionization emission lines are also very spatially extended and so not obviously related to an AGN broad- or narrow-line region. Once we reconsidered these cooling flow clusters, most were found to be too extended to harbor point sources luminous enough to be members of the EMSS sample on their own; but four clusters could not be so eliminated and so remain as potential (but not proven to be) BL Lac objects. These are MS 0102.3+3255, MS 1244.2+7114, MS 1455.0+2232 & MS 2348.0+2913. So, while it was the intention of this study to complete the M91 BL Lac sample, these four clusters were not observed with the HRI and so the M91 BL Lac sample may, indeed, contain a few more low-luminosity BL Lacs.

Nevertheless, our results generally agree with the predictions of BM93. The properties of the low-luminosity BL Lacs we have discovered are consistent with the low-luminosity BL Lacs predicted. And at the relatively bright flux limit of the M91 sample, MB95 predict very few low-luminosity BL Lacs would be misidentified, as we have found. Thus the B-M effect does not explain the $\langle V/V_{max} \rangle$ discrepancy between the M91 EMSS sample and 1Jy BL Lac sample, even if all four of the cooling flow clusters are included in the M91 BL Lac sample.

The properties of the newly discovered BL Lacs are suggestive of a transition population between BL Lacs and FR-1 radio galaxies, however their properties are too similar to that of the other BL Lacs in the EMSS sample to completely “bridge the gap” between XBLs and standard FR-1s in all their properties. But based upon this small study, surveys with significantly larger sky area and similar sensitivity (e.g., the RASS) will likely find numerous examples of low-luminosity BL Lacs whose properties are continuous between luminous X-ray selected BL Lacs, as found in the EMSS and Slew surveys, and normal FR-1 radio galaxies like M87. Indeed, the RGB (Laurent-Muelheisen et al. 1999) and Deep X-Ray Radio Blazar Survey (DXRBS; Perlman et al. 1998) surveys have found significant numbers of BL Lacs within this gap. These fainter surveys are also more susceptible to the problem of recognition of low-luminosity BL Lacs at low redshift, thus allowing for a more definitive test of the B-M effect.

Finally, the confirmation of IC 310 and 3C 264 as low-luminosity BL Lac objects suggests that other, nearby X-ray luminous clusters could harbor low-luminosity BL Lacs (similar to the case presented here for MS 0011.7+0837). Since many X-ray luminous clusters at $z < 0.1$ were targeted by the *Einstein* IPC, the EMSS would not have included these sources. However, the spectral results of Owen, Ledlow & Keel (1996),

which included enormous numbers of nearby Abell cluster radio galaxies, suggests that the numbers of low-luminosity BL Lacs in rich clusters is quite small. Still, ROSAT HRI images of suspect radio galaxies in nearby rich clusters, particularly the “cooling flow” clusters, should be targeted as potential BL Lac objects (e.g., 1005+006 & 1442+195 from the Owen et al. list). Similarly, HRI (or AXAF HRC) observations should be obtained for the five $z < 0.2$ BL Lac candidates discovered in Marchā et al. (1996) which exceed the W_λ , $D(4000)$ criteria of Stocke et al. (1991). Their (α_{ox} and α_{ro}) values, once corrected for the presence of the host galaxy, could confirm their classification as BL Lac objects, thus accounting for the marked absence of BL Lacs at $z < 0.2$.

This work was supported by NASA ROSAT grant NAG5-4518 and NASA LTSA grant NAGW-2645. The authors thank Simon Morris for the use of the optical spectrum of MS 1205.7-2921 and Isabella Gioia for the use of the optical spectrum of MS 1209.0+3917. We also thank Kohji Morikawa and Makoto Hattori for communicating their results on MS 1333.3+1725 prior to publication. We thank the referee for his or her intriguing idea that “cooling flow” clusters could harbor BL Lac objects. This research has made use of data obtained through the High Energy Astrophysics Science Archive Research Center Online Service, provided by the NASA/Goddard Space Flight Center as well as NASA’s Astrophysics Data System Abstract Service.

REFERENCES

Abraham, R.G., Crawford, C.S. & McHardy, I.M. MNRAS 1991 252, 482.
 Antonucci, R.R.J. & Ulvestad, J.S. 1985 ApJ 294, 158. (AU85)
 Bade, N., Beckmann, V., Douglas, N.G., Barthel, P.D., Engels, D., Cordis, L., Nass, P. & Voges, W. 1998 A&A, in press.
 Blair, A.J., Georantopoulos, I. & Stewart, G.C. 1997 MNRAS 289, 921.
 Browne, I.W.A. & Marchā, M.J.M. 1993 MNRAS 261, 795. (BM93)
 Condon, J.J., Cotton, W.D., Greisen, E.W., Yin, Q.F., Perley, R.A., Taylor, G.B. & Broderick, J.J. 1998 AJ, in press.
 Dahlem, M. & Stuhrmann, N. 1998 A&A 332, 449.
 Della Ceca, R. 1993, PhD dissertation, Johns Hopkins Univ.
 Dressler, A. & Shectman, S.A. 1987 AJ 94, 899.
 Ellingson, E. & Yee, H.K.C. 1994 ApJS 92, 33.
 Fabian, A.C. 1994 Ann. Revs. A. & Ap. 34, 32, 277.
 Ghisellini, G. & Maraschi, L. 1989 ApJ 340, 181.
 Gioia, I.M., Maccacaro, T., Schild, R.E., Wolter, A., Stocke, J.T., Morris, S.L. & Henry, J.P. 1990 ApJS 72, 567.
 Gioia, I.M. & Luppino, G.A. 1994 ApJS 94, 583.
 Giommi, P., Menna, M.T. & Padovani, P. 1998, in BL Lac Phenomenon (PASP conference series), in press.
 Giommi, P. & Padovani, P. 1994 MNRAS 268, 51.
 Heidt, J. & Wagner, S.J. 1996 A&A 305, 43.
 Jannuzzi, B.T., Smith, P.S. & Elston, R. 1993 ApJS 85, 265.
 Jannuzzi, B.T., Smith, P.S. & Elston, R. 1994 ApJ 428, 130.
 Kühr, H., Witzel, A., Pauliny-Toth, I.I.K. & Nauber, U. 1981 A&AS 45, 367.
 Laurent-Muehleisen, S.A., Kollgaard, R.I., Moellenbrock, G.A. & Feigelson, E.D. 1993 AJ 106, 875.
 Laurent-Muehleisen, S.A., Kollgaard, R.I., Feigelson, E.D. & Brinkmann, W. 1998, in prep.
 Lewis, A.D., Stocke, J.T., Ellingson, E. & Gioia, I.M. 1998, in prep.
 Maccacaro, T., Wolter, A., McLean, B., Gioia, I.M., Stocke, J.T., Della Ceca, R., Burg, R. & Faccini, R. 1994 Astro Lett. & Comm. 29, 267.
 Marchā, M.J.M. & Browne, I.W.A. 1995 MNRAS 275, 951. (MB95)
 Marchā, M.J.M., Browne, I.W.A., Impey, C.D. & Smith, P.S. 1996 MNRAS 281, 425.
 Morris, S.L., Stocke, J.T., Gioia, I.M., Schild, R.E., Wolter, A. & Della Ceca, R. 1991 ApJ 380, 49. (M91)
 Morrison, R. & MacCammon, D. 1983 ApJ 270, 119.
 Morse, J.A. 1994 PASP 106, 675.
 Nass, P., Bade, N., Kollgaard, R.I., Laurent-Muehleisen, S.A., Reimers, D. & Voges, W. 1996 A&A 309, 419.
 Owen, F.N., Ledlow, M.J. & Keel, W.C. 1996 AJ 111, 53.
 Padovani, P. & Urry, C.M. 1990 ApJ 356, 75.
 Padovani, P. & Giommi 1996 MNRAS 279, 526.
 Perlman, E.S. & Stocke, J.T. 1993 ApJ 406, 430.
 Perlman, E.S., Stocke, J.T., Wang, Q.D. & Morris, S.L. 1996a ApJ 456, 451.
 Perlman, E.S., Stocke, J.T., Schachter, J.F., Elvis, M., Ellingson, E., Urry, C.M., Potter, M., Impey, C.D. & Kolchinsky, P. 1996b ApJS 104, 251.
 Perlman et al. 1998 AJ 115, 1253.
 Prieto, M.A. 1996 MNRAS 282, 421.
 Rector, T.A. & Stocke, J.T. 1999, in prep.
 Rector, T.A., Stocke, J.T., Perlman, E.S., Morris, S.L. & Gioia, I.A. 1999, in prep.
 Rhee, G., Burns, J.O. & Kowalski, M.P. 1994 AJ 108, 1137.
 Sambruna, R.M., Urry, C.M., Ghisellini, G. & Maraschi, L. 1995 ApJ 449, 567.
 Stickel, M., Padovani, P., Urry, C.M., Fried, J.W. & Kühr, H. 1991 ApJ 374, 431
 Stickel, M., Fried, J.W. & Kühr, H. 1993 A&AS 98, 393.
 Stocke, J.T., Morris, S.L., Gioia, I.M., Maccacaro, T., Schild, R.E. & Wolter, A. 1989, in BL Lac Objects, ed. L. Maraschi, T. Maccacaro & M.-H. Ulrich (Heidelberg: Springer-Verlag), 242.
 Stocke, J.T., Morris, S.L., Gioia, I., Maccacaro, T., Schild, R.E., & Wolter, A. 1990 ApJ348, 141.
 Stocke, J.T., Morris, S.L., Gioia, I.M., Maccacaro, T., Schild, R., Wolter, A., Fleming, T.A. & Henry, J.P. 1991 ApJS 76, 813.
 Stocke, J.T., Perlman, E.S., Gioia, I.M. & Harvanek, M. 1999 AJ, submitted.
 Stocke, J.T. & Rector, T.A. 1997 ApJ 489, L17.
 Stocke, J.T., Rector, T.A. & Griffiths, R.W. 1999, in prep.
 White, R.L., Becker, R.H., Helfand, D.J. & Gregg, M.D. 1997 ApJ 475, 479.
 Wurtz, R., Stocke, J.T. & Yee, H.K.C. 1996 ApJS 103, 109.
 Zensus, J.A. 1989, in BL Lac Objects, ed. L. Maraschi, T. Maccacaro & M.-H. Ulrich (Heidelberg: Springer-Verlag), 3.

TABLE 1
LOG OF ROSAT HRI OBSERVATIONS

Object	ROR#	Date	Exposure	M91?	RA (B1950) ^a	Dec
MS 0011.7+0837	RH701839	4 Jan 1995	6848	Y	00:11:45.3	+08:37:24.3
MS 0433.9+0957	RH701840	3 Mar 1995	7530	Y	04:33:57.2	+09:56:48.3
MS 1004.2+1238	RH702864	16 May 1997	7374	Y	10:04:12.5	+12:38:22.1
MS 1019.0+5139	RH600125	26 Oct 1991	7190	Y	10:19:03.5	+51:39:09.1
MS 1050.7+4946	RH701841	2 Dec 1994	2895	Y	10:50:47.6	+49:45:51.7
MS 1154.1+4255	RH701843	21 May 1995	6243	N	11:54:11.6	+42:54:52.1
MS 1205.7-2921	RH702867	3 Jan 1997	10651	N	12:05:43.2	-29:21:18.3
MS 1209.0+3917	RH701844	18 May 1995	11355	N	12:09:02.9	+39:17:35.9
MS 1317.0-2111	RH702865	1 Aug 1997	8491	N
MS 1520.1+3002	RH702866	15 Jul 1997	10549	N	15:20:11.4	+30:05:38.3 ^c
MS 1826.5+7256	RH600124	12 Sep 1991	36803	Y	18:26:25.1	+72:56:10.2
MS 2301.3+1506	RH701842	20 Dec 1994	7287	Y	23:01:16.7	+15:06:53.2

^aFor extended sources, the position marks the peak flux.

^bNo sources are detected within the HRI field.

^cPosition of northern source. Does not coincide with radio source (see discussion of this source in §5).

TABLE 2
X-RAY PROPERTIES OF BL LAC CANDIDATES

Object	M91?	$\log nH$ (cm^{-2})	α_x	f_{HRI}	$\log L_{HRI}$ (erg s^{-1})	f_{IPC} ($\alpha_x = 1$)	f_{IPC} ($\alpha_x = \text{Col. 4}$)	% ^a
0011.7+0837	...	20.79	1.73	6.71	43.94	13.11	16.46	17%
1019.0+5139	Y	19.98	0.56	47.8	44.67	13.28	17.06	298%
1050.7+4946	Y	20.11	1.62	26.3	44.40	14.09	8.86	136%
1154.2+4255	N	20.15	1.68	5.35	43.89	4.04	2.72	86%
1205.7-2921	N	20.76	1.48	21.4	44.86	3.23	3.78	296%
1209.0+3917	N	20.32	0.74	5.47	45.15	2.83	2.39	146%

^aRatio of ROSAT HRI to *Einstein* IPC flux. See text for a full description.

^bThis object is not identified as a BL Lac (see text).

TABLE 3
OPTICAL AND RADIO PROPERTIES OF BL LAC CANDIDATES

Object	z	V	W_λ	$D(4000)$	S_{core}	S_{ext}	S_{tot}	f	$\log L_{core}$	$\log L_{ext}$
0011.7+0837 ^a	0.162	17.50	≤ 2.1	1.43 ± 0.17	47.1	219	266	0.21	24.75	25.35
1019.0+5139 ^b	0.141	18.09	3.3	1.30 ± 0.15	3.1	≤ 0.6	3.1	≥ 5.3	23.44	≤ 22.67
1050.7+4946 ^b	0.140	16.86	2.5	1.47 ± 0.09	52.8	13.2	66.0	4.0	24.67	24.01
1154.2+4255 ^c	0.170	17.67	≤ 3.0	1.50 ± 0.23	12.6	4.8	17.4	2.6	24.22	23.73
1205.7-2921 ^d	0.249	17.50	≤ 4.0	1.64 ± 0.45	4.4
1209.0+3917 ^c	0.616	20.00	≤ 4.5	1.17 ± 0.17	12.1	≤ 2.0	12.1	≥ 30	25.39	24.38

^aVLA 20cm A-array (mJy)

^bVLA 20cm B-array (mJy)

^cVLA 20cm B-array (mJy; FIRST survey; White et al. 1997)

^dVLA 6cm C-array (mJy; Stocke et al. 1991)

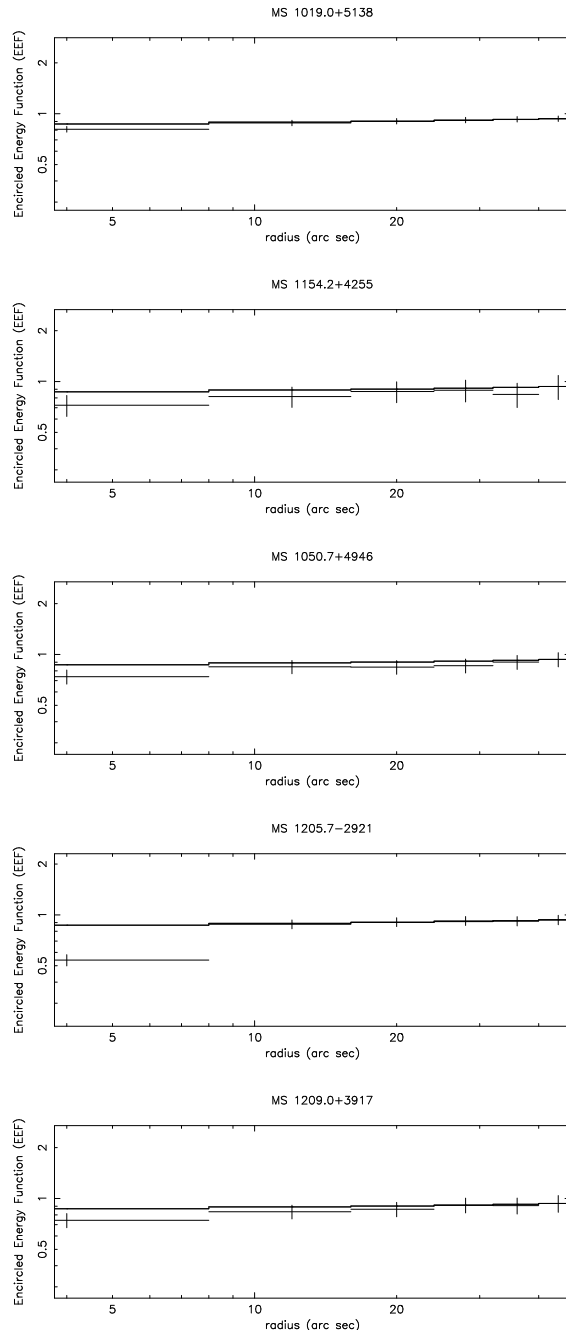


FIG. 1.— The radial energy profile (data points with 1σ error bars) for the unresolved sources plotted against the Encircled Energy Function (EEF; solid lines) for the ROSAT HRI. The object's EEF is normalized to the HRI point-source EEF at a radius of $50''$. Note that each source does not match exactly the EEF at a radius of $\leq 8''$. This is due to an “excess halo” at $\sim 10''$, which is also present for stars within the field; so that these objects are completely consistent with being unresolved sources.

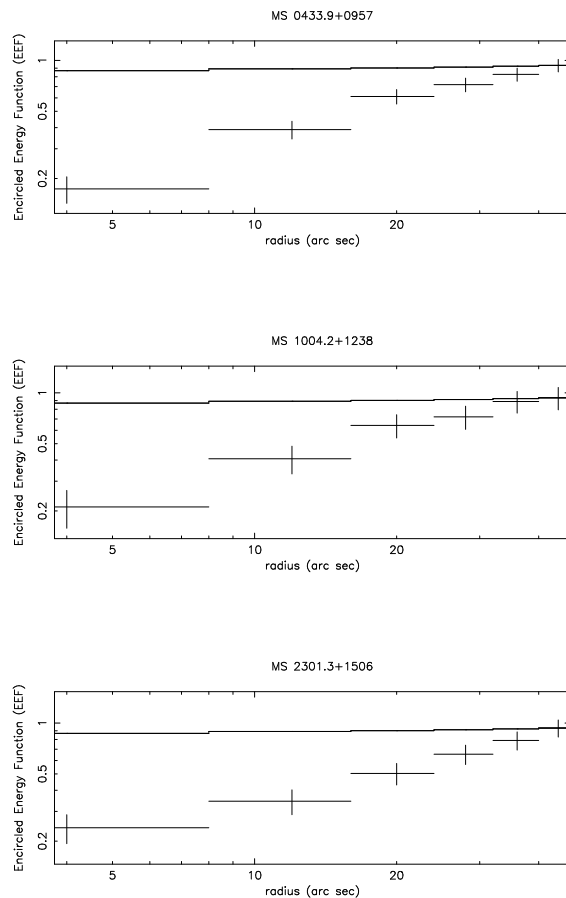


FIG. 2.— The radial energy profile (data points with 1σ error bars) for the resolved sources plotted against the Encircled Energy Function (EEF; solid lines) for the ROSAT HRI (see Figure 1 for a full description of the EEF). Each object's total flux is dominated by the extended flux, thus causing the energy profile to lie well below the HRI EEF at small and large radii, not just at $\leq 8''$ where the objects in Figure 1 exhibit the “excess halo.”

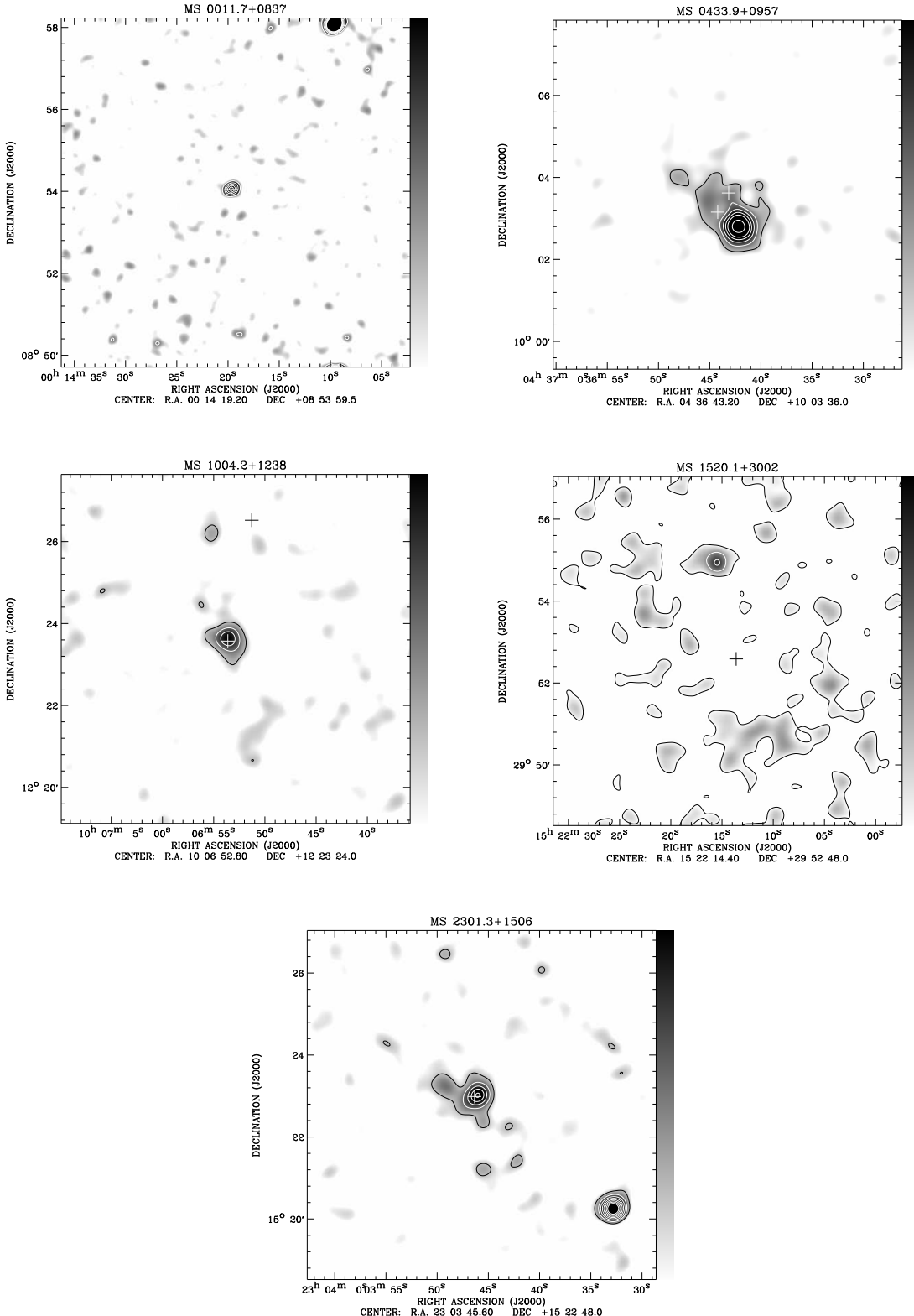


FIG. 3.— Contoured, logarithmic grey-scale X-ray maps of the resolved sources. For all sources the greyscale is logarithmic from 0.015 to 0.05 counts arcsec^{-1} . The map for MS 0011.7+0837 is smoothed by a Gaussian kernel equivalent to the on-axis point-spread function (PSF) of the HRI. The other maps are smoothed by a Gaussian twice the width of the HRI PSF to enhance the extended flux. The contour levels for the map of MS 0011.7+0837 are linearly increasing from 0.03 in 0.03 increments (in counts arcsec^{-1}). For the other maps the contours linearly increase from 0.02 in 0.01 increments. The positions of radio galaxies within the field are marked with crosses. Further discussion of individual maps can be found in §5.

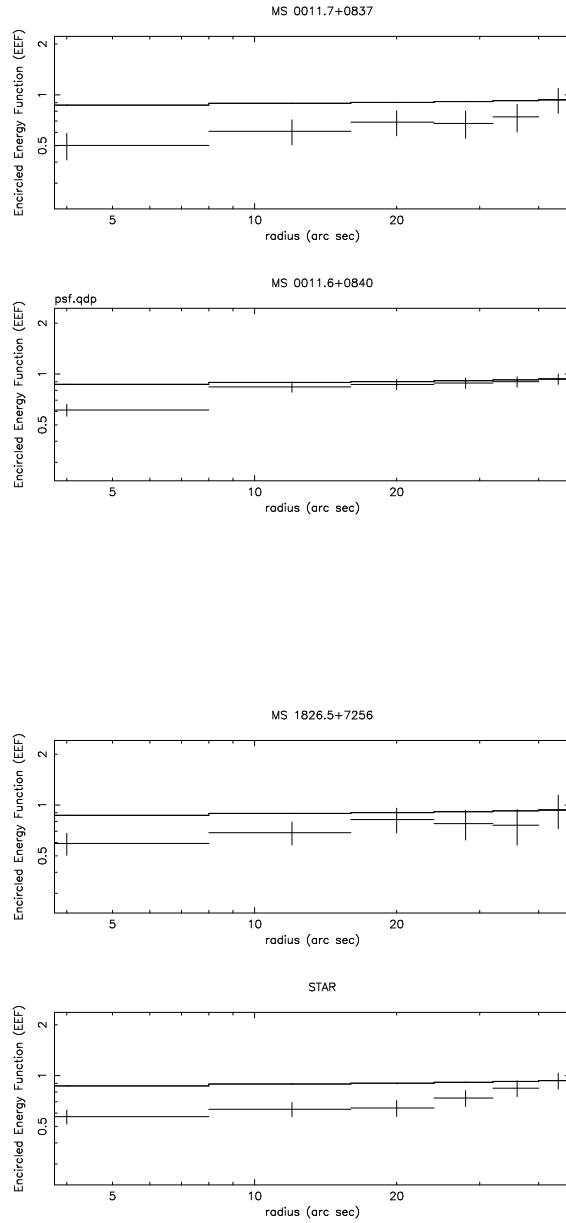


FIG. 4.— The radial energy profiles for MS 0011.7+0837 and MS 1826.5+7256 as well as for in-field stars plotted against the point-source EEF for the ROSAT HRI (see Figure 1 for a full description of the EEF). The radial energy profile for MS 0011.7+0837 is not consistent with the nominal HRI EEF, whereas the in-field star MS 0011.6+0840 does match the HRI EEF (excepting the “excess halo” described in §3). The probability that the energy profile of MS 0011.7+0837 is the same as MS 0011.6+0840 is $\sim 1\%$ (the variance summed over all the annuli is $\sigma = 3.77 \pm 0.27$). In contrast, the radial energy profiles for MS 1826.5+7256 and its in-field star are not consistent with the HRI EEF; however, the radial energy profile for MS 1826.5+7256 is completely consistent with that of the star; the probability is $> 95\%$ that they are the same ($\sigma = 0.01 \pm 0.34$). This suggests that MS 1826.5+7256 is unresolved, but that an as yet unexplained problem with the observation exists. Excessive jitter due to the length of the exposure is a possible explanation.

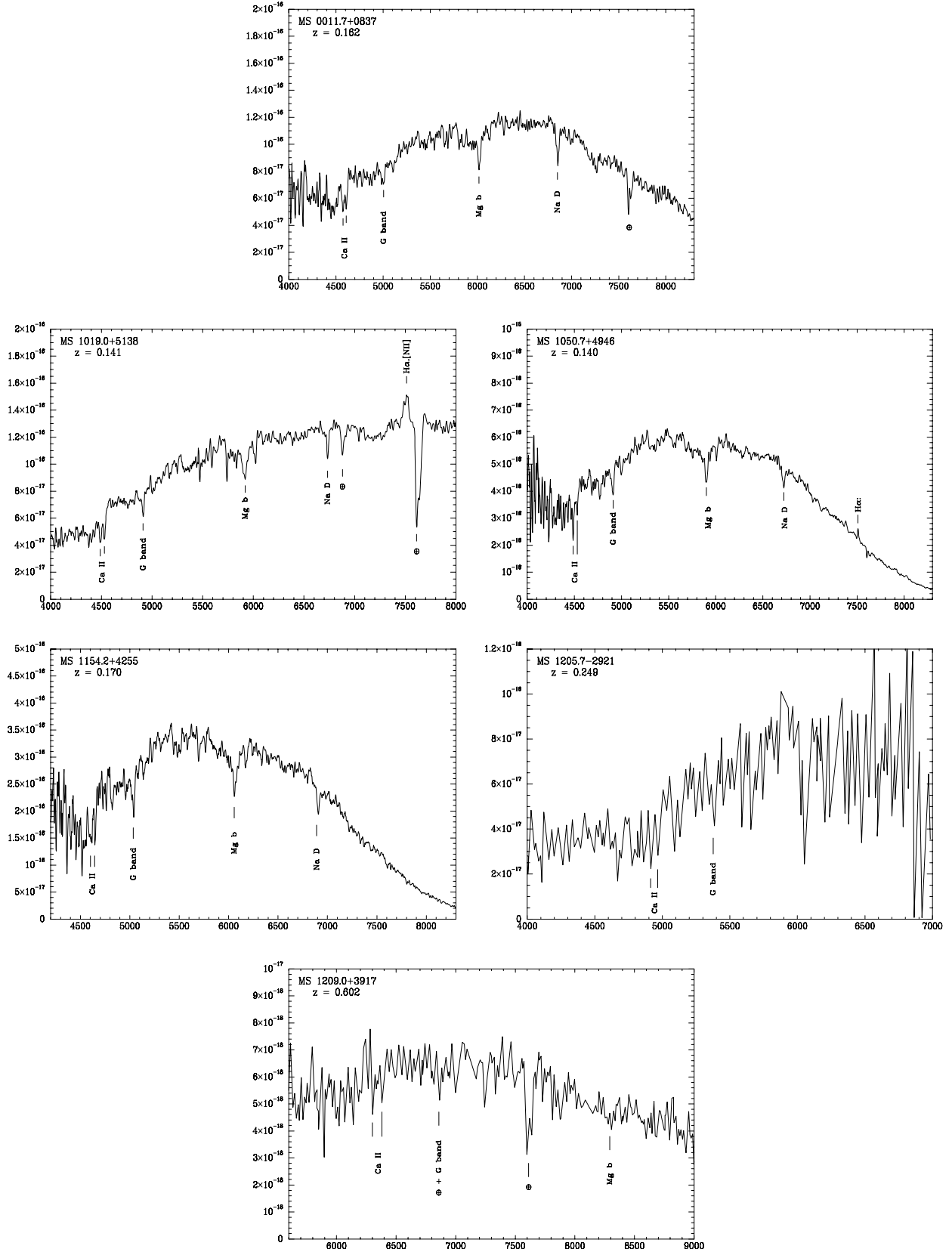


FIG. 5.— Optical spectra of the BL Lac candidates and the radio galaxy in MS 0011.7+0837. The flux scale is F_λ in $\text{ergs s}^{-1} \text{cm}^{-2}$; the x-axis is wavelength in \AA . The symbol \oplus identifies features due to the Earth's atmosphere. Due to the small slit width ($2''$) these fluxes are only approximate, although the relative fluxes shortward of 6500\AA are reasonably correct. Longward of 6500\AA the flux calibration is incorrect due to second-order overlap for all spectra except MS 1019.0+5138.

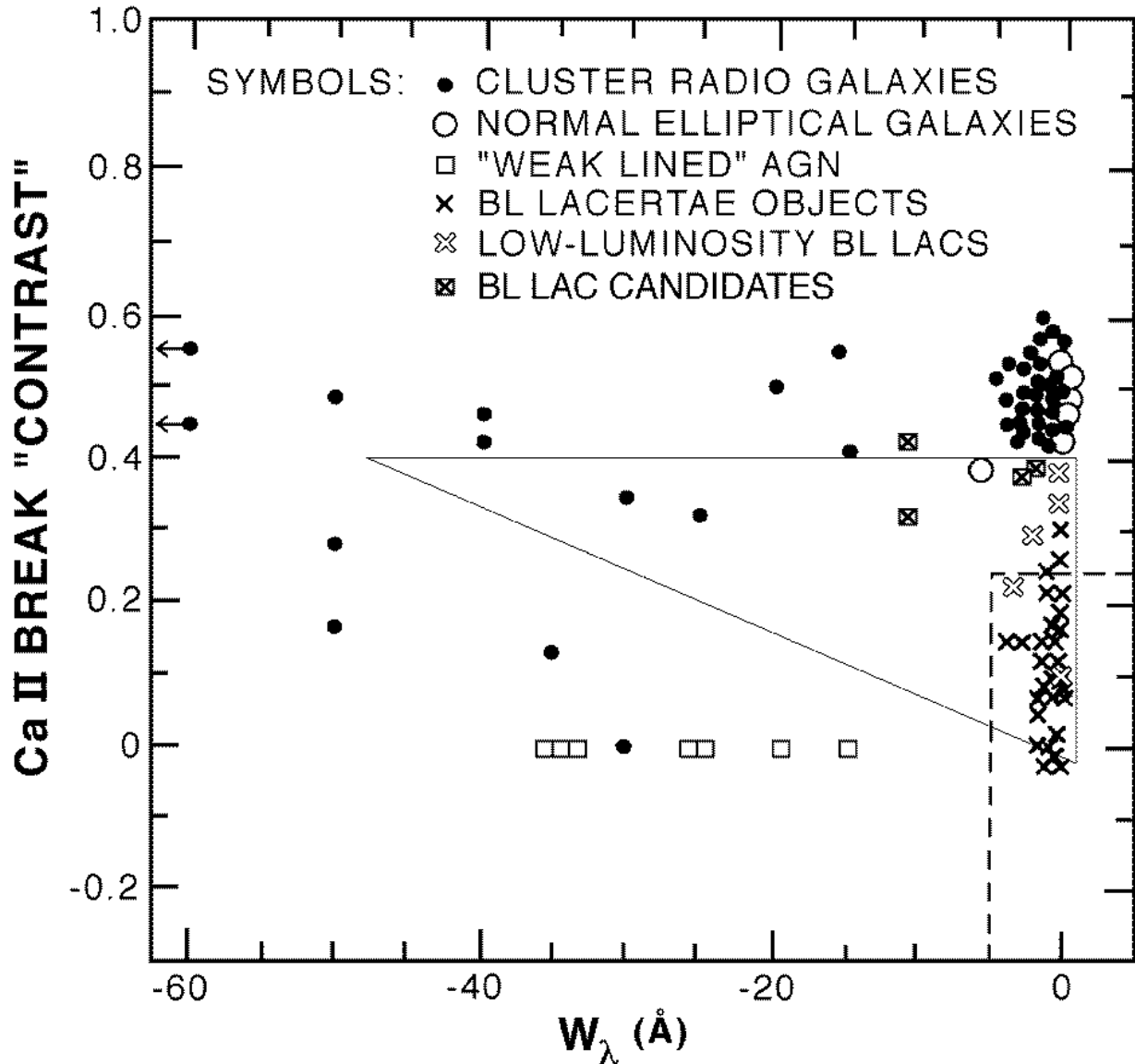


FIG. 6.— CaII break “contrast” vs. equivalent width (W_λ) for a sampling of extragalactic EMSS objects. This plot (adapted from Stocke et al. 1991) uses the largest W_λ of any emission line present and the break “contrast” at CaII H&K (defined as the relative flux depression across the H&K break ($= [f(4000\text{\AA}^+) - f(4000\text{\AA}^-)/f(4000\text{\AA}^+)]$)). The subregion which meets the BL Lac classification criteria suggested by Stocke et al. (1991) is shown in dashed lines; i.e., $W_\lambda \leq 5\text{\AA}$ and a break contrast $\leq 25\%$ ($D(4000) \leq 1.33$; Dressler & Shectman 1987). Note that three of the new “low-luminosity” BL Lacs, along with the BL Lac MS 2306.1-2236, have stronger H&K contrasts than this criterion. These objects however do match the BL Lac criteria proposed by March{\`a} et al. (1996; solid lines). Three of the four BL Lac candidates of Owen, Ledlow & Keel (1996) also fall within this region; however we note that very few BL Lac-like objects in the EMSS are detected within this triangular region but outside the region considered herein for BL Lac objects.

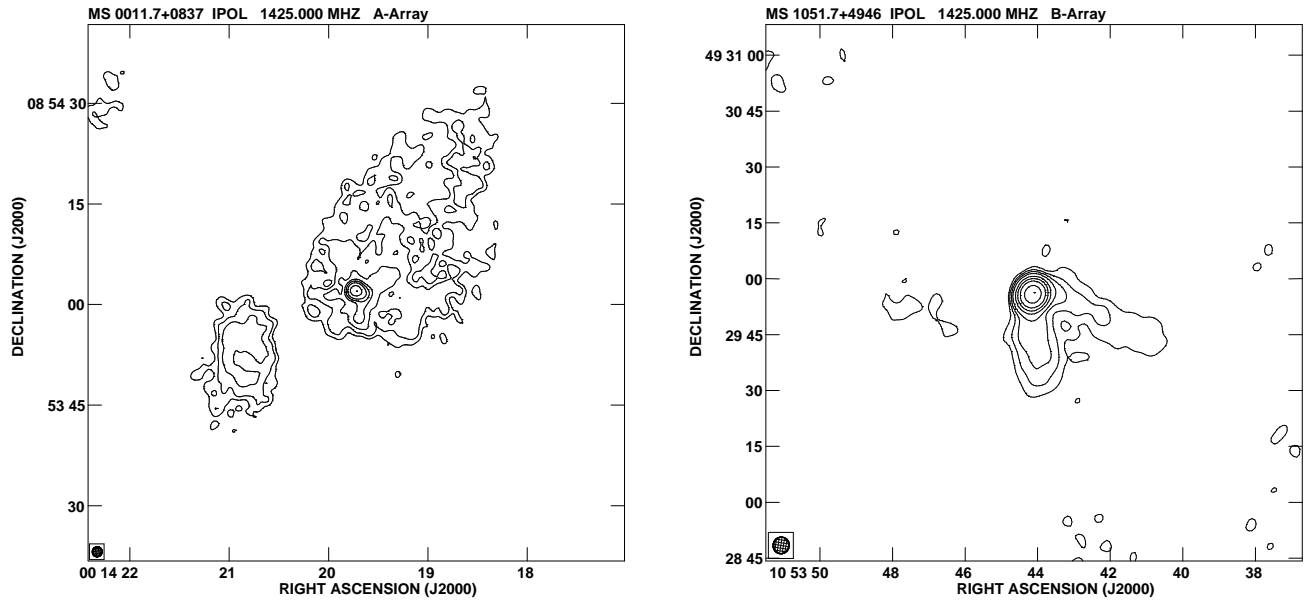


FIG. 7.— VLA 20cm radio maps of MS 0011.7+0837 (A-array) and MS 1050.7+4946 (B-array). The base level of each map is set roughly at the 2σ RMS noise level. For MS 0011.7+0837 the peak flux is 47.8 mJy; and the contours are 0.5, 1, 2, 5, 10, 20, 50 and 100% of the peak flux. For MS 1050.7+4946 the peak flux is 49.4 mJy; and the contours are 0.2, 0.5, 1, 2, 5, 10, 20, 50 and 100% of the peak flux. The beam is shown in the lower left. A map of MS 1019.0+5139 is not shown as extended flux was not detected for this source at 20cm in either A- or B-array.

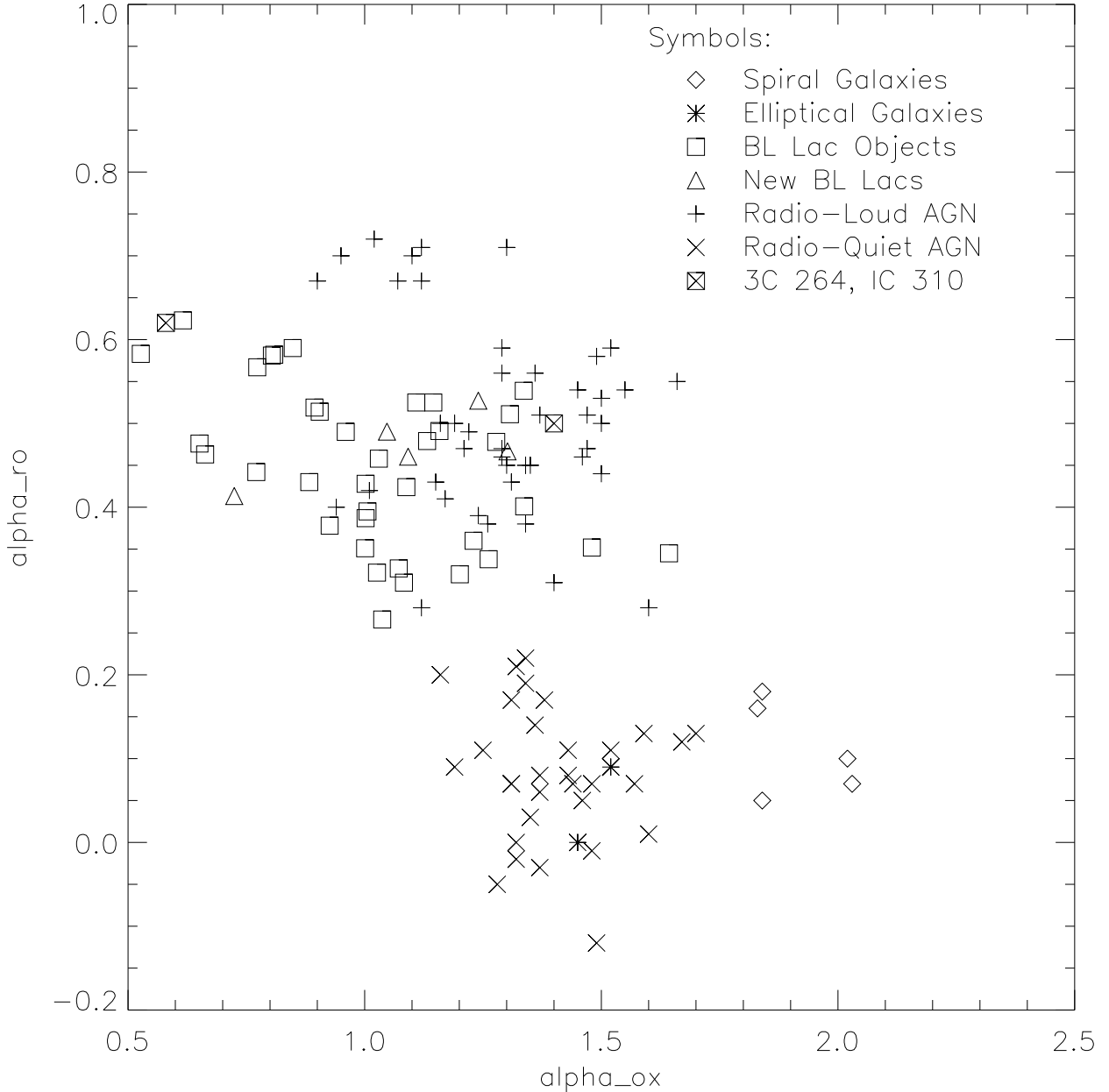


FIG. 8.—Overall energy distributions for extragalactic sources in the EMSS which were detected at 6cm (Stocke et al. 1991). The axes are the radio-to-optical and X-ray-to-optical spectral indices (α_{ro} and α_{ox} respectively) as defined in Stocke et al. (1991). Radio-loud objects are at the top of the plot and X-ray-loud objects are to the left. The newly discovered BL Lac objects (shown as triangles) have similar (α_{ox} , α_{ro}) values as compared to the other EMSS BL Lacs. The (α_{ox} , α_{ro}) values for all of the EMSS BL Lacs as well as the radio galaxies 3C 264 and IC 310 have been corrected to account for the presence of the host elliptical galaxy (see §4 for a description). Note that BL Lacs and radio-loud AGN lie in a region of this plot relatively distinct from the radio-quiet AGN and normal elliptical galaxies.